Reprinted from

IEEE Computer Society Conference on Pattern Recognition and Image Processing

June 1982

Resolution Matching for Registration of Dissimilar Images

by Paul E. Anuta and Farzin Davallou

Reprinted from PROCEEDINGS OF THE IEEE COMPUTER SOCIETY
CONFERENCE ON PATTERN RECOGNITION AND IMAGE PROCESSING, June 1982

RESOLUTION MATCHING FOR REGISTRATION OF DISSIMILAR IMAGES

Paul E. Anuta
Farzin Davallou

Laboratory for Applications of Remote Sensing
Purdue University
West Lafayette, IN 47906-1399

ABSTRACT

The problem of matching remote sensing image data from different sensors is discussed. The image data can differ in spectral characteristics and in resolution. The specific example of RBV imagery and MSS imagery from the Landsat-3 satellite is considered. Resolution matching is implemented using cubic polynomial interpolation and IFOV deconvolution. Spectral characteristic matching was done by band combination. Registration error variance reduction was implemented using a gradient process. Results are presented for RBV/MSS data from a typical terrain scene. Significant reduction in edge width is observed when IFOV deconvolution is applied to the low resolution data. Correlation results show higher coefficient of correlation and greater percentage of acceptable correlations when deconvolution is used.

I. INTRODUCTION

In many remote sensing image data applications, it is beneficial to combine data from different sensors. Often the characteristics of the sensors are quite different and achieving precise registration of the different data types is a challenging problem. The case considered in this paper is one in which the resolution of two imaging sensors is significantly different and the nature of the image is only moderately different. Specifically, we are concerned with multispectral images in the optical and near infrared portion of the spectrum obtained from satellite platforms. The imagery studied is from the Landsat-3 MSS and RBV sensors. The MSS has a nominal resolution of 80 meters and the RBV resolution is 20 to 40 meters. Any similar combination of reflectance spectra-measuring sensors with differing resolutions would be appropriate for the results of this study. One other sensor pair example is the planned SPOT system the French plan to launch in 1984 and the U.S. Thematic Mapper sensor scheduled for launch in July 1982. The SPOT system is to have a panchromatic band resolution of 10 meters and the NASA system will have 30 meter resolution. Other examples of low-resolution multispectral sensors exist and in many cases it would be desirable to combine these data with a higher-resolution sensor. The primary impetus for this is to observe scene structure in the high-resolution imagery and to obtain spectral measurements from the scene using the lower-resolution multispectral sensors.

The problem is first addressed from the theoretical point of view in which an optimum filter is determined that will minimize the variance of the registration estimate. This solution is then implemented along with other methods and compared using test data from the Landsat system.

II. REGISTRATION PROCESSOR

A model which represents this registration case is shown in Figure 1. It is assumed that the input is a high-resolution image and the lower-resolution image is generated by convolving an IFOV function with the high-resolution image. Then preprocessing filters are applied to the two images and the results correlated to produce estimates of misregistration. There are three parts to the problem as modeled here. The first is to deconvolve the effect of the IFOV. The second is to resample the low-resolution image to produce the resolution to match the high-resolution image. The third is to optimize the registration performance, given a particular model. Solutions to the first are numerous in the literature and particular examples are given by Riemer[1], Chu[2], and Dye[3]. In any case, a filter is defined which is convolved with the image to correct for the effect of the IFOV. The second problem is solved here by using cubic polynomial interpolation in conjunction with the IFOV deconvolution. For the third problem, the objective is to minimize the variance of the registration estimate and many authors (Svedlow[4]) have observed that the matched filter is the optimum processor. This is characterized by a whitening filter to remove the effects of the noise and cross correlation of the preprocessed images. The whitening filter used here is based upon the noise statistics for the difference between the images to be registered. We have observed[4] that the Landsat imagery has an approximately negative exponential correlation function. This leads to a whitening filter of the form:

$$h_w(x,y) = \frac{1}{2A\sqrt{\alpha\beta}}\left[\alpha\beta\delta(x,y) + \beta\frac{1}{dx} + \alpha\frac{d}{dy} + \frac{d^2}{dxdy}\right]$$

The optimum result is a linear processor and assumes that the processor is continuous. In most applications, image data are quantized to six to seven bits and are processed in sampled form, i.e., a digital image. Furthermore, in order to reduce processing costs, it is desirable to convert the image to a binary image and use logical comparison and summing for correlation rather than floating-point multiplication and addition as is needed for the continuous correlation function. The conversion to a binary image is done by thresholding the image at some value which converts the problem to a nonlinear one and introduces another parameter. The original image can be thresholded, the filtered image can be thresholded, or variations of the preprocessed image can be thresholded.

An interesting transformation of the form of the preprocessor takes place at this point. The derivative preprocessor comes about from the optimum solution because the inverse of the noise power spectral density appears in the solution to whiten the correlation function and produce a sharper correlation peak. The derivative also is the method used to enhance edges in a scene; thus, the optimum solution can be looked at as an edge-enhancement result. Then thresholding the preprocessed image to reduce computation also is the operation which in effect classifies the image into an edge, no-edge image. Thus, one starts with a linear prewhitening operation and ends up with what is in effect an edge-detection and correlation process. It is not clear that the edge detection and correlation also is an optimum solution and would give the same error variance as the linear optimum solution.

We have discussed the third aspect of the dissimilar image registration problem thus far. Increasing the resolution of the lower resolution image can be carried out by deconvolving the effect of the IFOV and interpolating to a higher sample rate. Several solutions to the deconvolution problem are available as cited above. Results have been observed to be similar for filters designed by different methods using different assumptions. We have used here a solution based on the assumption of a Gaussian-shaped IFOV with a radius of gyration of 80 meters and a resolution improvement ratio of one half. As noted above, cubic interpolation is combined with this filter to produce the resolution-enhancement filter. The filter has the shape shown in Figure 2. The resulting preprocessing filters are then:

$$h_1(x,y) = h_D(x,y) \circledast h_w(x,y)$$

$$h_2(x,y) = h_w(x,y)$$

where:

$h_w(x,y)$ is a prewhitening filter which is the reference image invariant part of the matched filter

$h_D(x,y)$ is the IFOV deconvolution filter combined with cubic resampling.

III. TEST DATA SETS

Registration tests were run on test data from an area near Fort Dodge, Iowa. RBV and MSS test data could not be obtained for the same day due to data acquisition problems. However, a very close match was obtained from overlap coverage nine days separate in time. The RBV data are from Frame 830922-16095 on September 12, 1980 and the MSS data are from Frame 27051-16204 on September 3, 1980. The MSS data are of good quality but the RBV data are of lower quality than expected. The RBV data have a pronounced speckled effect due to telemetry and ground-processing problems and because the signal-to-noise ratio was low. Also, shading was apparent from place to place over the subframe. These data are the best available with MSS data.

The MSS IFOV is nominally 80 meters. These data are sampled to have nominally 57 meter square pixels in the Landsat-3 data. The RBV data have nominally 19 meter pixels with the actual resolution being in the area of 40 meters. In order to match resolutions for registration without deconvolution, the MSS data were first interpolated using cubic interpolation by a factor of three to produce 19 meter pixels. This is a low-cost method of achieving the higher pixel resolution and it was of interest to test this approach since the IFOV deconvolution methods discussed above are more costly. Figure 3 contains a photographic reproduction of a dot printer grayscale image of the RBV data for the test area. The field and road structure is clearly evident. Figure 4 is a dot printer reproduction for MSS Band 5 cubic interpolated to 19 meter pixels. Figure 5 is the same for Band 6. Note the much broader width of roads and field edges.

IV. EXPERIMENTAL EVALUATION

The three images shown form the basis for experimental results. Although the optimum correlator solution indicates that the best preprocessor is a gradient operator feeding a linear correlator, practical considerations dictate that binary or edge no-edge correlators be used in actual implementations due to computing-cost considerations. Thus the test images were processed with a gradient type preprocessor and the magnitude of the result was thresholded to produce a 0-1 binary edge image. Results of other researchers indicate that the Sobel gradient edge operator is very effective and, at the same time, low cost [5]. Thus the Sobel operator was chosen to implement the gradient function. The edge threshold was chosen by examining edge histograms and choosing samples from edge areas. The threshold places 10 to 15% of the edge pixels above the threshold.

The problem of differing spectral bands of the two sensors was approached by combining edges from MSS Bands 5 and 6. The RBV spectral band is .5 to .75 μm, MSS Band 5 is .6 to .7 μm, and Band 6 is .7 to .8 μm. Combining Bands 5 and 6 is a reasonably good approximation. Roads tend to show up well in 5 and field edges are very strong in Band 6. The RBV image contains both clear roads and field edges. Figure 6 contains the edge image for the RBV data and Figure 7 contains the combined Band 5 and 6 edges, both using the Sobel gradient.

Correlation tests were run on the edge images using the correlation coefficient to enable a correlation number between -1 and 1 to be obtained. As noted above, in an operational implementation, a binary logic and counter arrangement would be used for maximum efficiency; but in the research stage, the more complex expression can be used. The non-thresholded data were also correlated to give a comparison with the thresholded case. The MSS Band 5 and Band 6 edges were not combined for these cases, so the correlations were done separately. Table 1 and Table 2 contain the results. The analysis assumes the scales are the same for the MSS and RBV, so the position of the correct shift peak in the correlation function would be the same in all tests. To verify this, a geometric analysis was made of the RBV versus MSS images. Three control points were accurately chosen in RBV and MSS printouts and an affine function was fit to these points. Three points provide six values so the six parameters can be computed. The affine form is:

$$x' = a + bx + cy \quad \text{(Lines)}$$

$$y' = d + ex + fy \quad \text{(Cols.)}$$

These six parameters provide specification of translation in two dimensions, rotation, scale in two dimensions, and skew. The results were a = 23, b = -109, and all others were zero. This verifies that there is no rotation, scale difference, or skew between the RBV and MSS imagery to six decimal places. The constant shift of 23 lines and -109 columns was used in all the correlations to place the correct peak at the center of the correlation function output.

The correlation results for thresholded RBV and combined MSS Band 5 and 6 edges are presented in Table 3. A slightly different evaluation method was used. If peaks were at the lag limit, they were not used and if a secondary peak was observed closer to the center (true) position, it was used instead of the primary peak. Errors in the region of three to four pixels could be expected using the preprocessing described.

Next, IFOV deconvolution operation discussed above was run on the MSS data to sharpen the edges. Figure 8 contains the thresholded Sobel edges for the deconvolved Band 6 data. Note the much narrower edges. Correlation tests with the RBV edges were conducted to see if results were improved. The correlation results are presented in Table 4. It can be seen that the line standard deviation is lower and the column value is about the same. However, the % acceptable was higher and the average correlation was much higher.

V. CONCLUSIONS

An experimental evaluation of gradient and deconvolution enhanced satellite imagery was discussed for registration of data having different spatial and spectral characteristics. Improvement in the narrowness of edges in the lower resolution imagery was observed and some improvement in correlation improvement was observed. The results indicate that it is potentially beneficial to use deconvolution to register dissimilar images; however, more extensive evaluation should be carried out using filters designed using different assumptions to optimize the quality of the enhanced image.

REFERENCES

1. Riemer, T.E.; C.D. McGillem, "Optimum Constrained Image Restoration Filters," LARS Information Note 091974, Laboratory for Applications of Remote Sensing (LARS), Purdue University, West Lafayette, IN, Sept. 1974.

2. Chu, N.Y.; C.D. McGillem, "Methods and Performance Bounds for Constrained Image Registration," LARS Technical Report 061678, June 1978.

3. Dye, R.H., "Restoration of Landsat Images by Discrete Two-Dimensional Deconvolution," Proc. of 10th Intl. Symp. on Remote Sensing of Environment, Ann Arbor, MI, Oct. 6-10, 1975.

4. Svedlow, M.E.; C.D. McGillem; P.E. Anuta, "Analytical and Experimental Design and Analysis of an Optimal Processor for Image Registration," LARS Information Note 090776, Sept. 1976.

5. Abdou, I.E.; W.K. Pratt, "Quantitative Design and Evaluation of Enhancement/Thresholding Edge Detectors," Proc. of IEEE, Vol. 67, No. 5, May 1979, pp. 753-763.

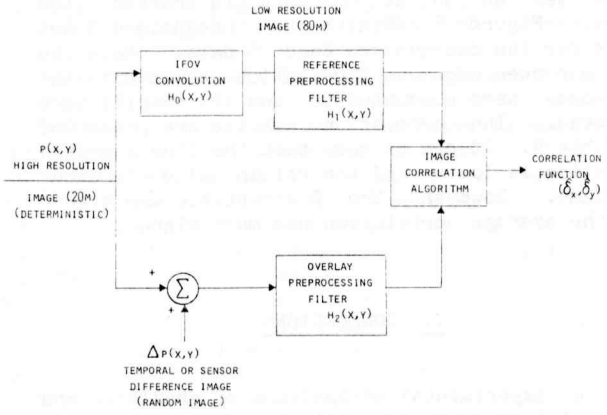

Figure 1. Model for analysis of registration with different resolutions.

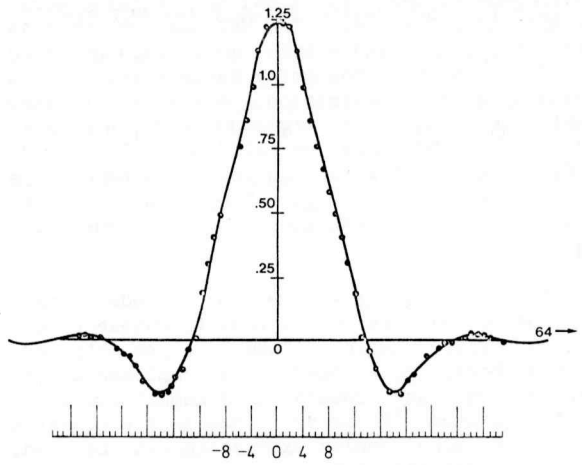

Figure 2. IFOV deconvolution filter example.

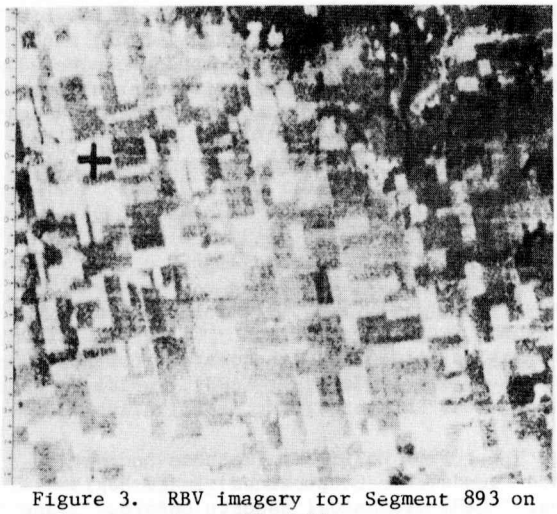

Figure 3. RBV imagery for Segment 893 on Sept. 12, 1980.

Figure 4. MSS Band 5 imagery interpolated to 19m using cubic interpolation. Sept. 3, 1980

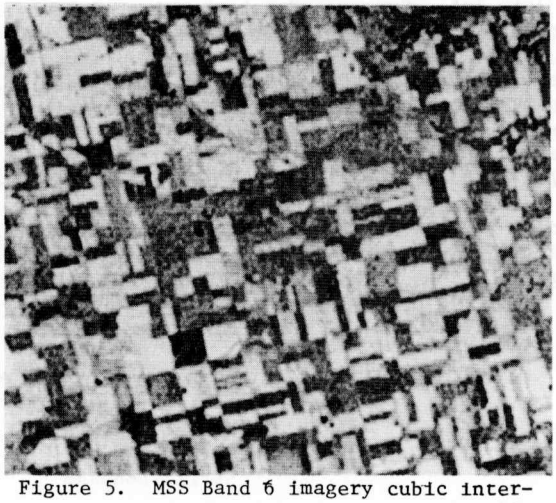

Figure 5. MSS Band 6 imagery cubic interpolated to 19m for data from Sept. 3, 1980.

Figure 6. RBV edge image obtained from thresholded Sobel gradient.

Table 1. Correlation Results for MSS Band 5 vs. RBV.
Non-Thresholded Sobel Edges

ρMAX	ΔL	ΔC	UNIQUE PEAK	ρMAX	ΔL	ΔC	UNIQUE PEAK
.29	-3	3	Yes	.14	-2	5	Yes
.17	-6	8	Yes	.16	7	2	No
.08	-7	2	No	.24	-8	-2	Yes
.08	-4	2	No	.07	-4	4	Yes
.22	1	6	No	.22	-8	2	Yes
.14	-2	4	Yes	.42	-2	3	Yes
.07	4	3	No	.08	-6	7	No
.14	-8	3	Yes	.13	-5	-6	No
.08	-4	2	No	.25	-8	2	Yes
.28	-7	4	No	.09	-4	3	No
.10	4	3	Yes	.10	-8	4	No
.10	-4	6	No	.03	-8	1	No
.11	-8	4	No	.42	-4	2	Yes
.30	-3	3	Yes	.09	-1	6	Yes
.12	1	4	Yes	[Mean ρ = .16]			

* For Unique Peak results only

	$\overline{\Delta L}$	$\overline{\Delta C}$
MEAN*	-3.6	3.33
STD*	3.94	2.12

% Acceptable: 52%

Table 2. Correlation Results for MSS Band 6 vs. RBV.
Non-Thresholded Sobel Edges

ρMAX	ΔL	ΔC	UNIQUE PEAK	ρMAX	ΔL	ΔC	UNIQUE PEAK
.25	-6	2	Yes	.20	-8	2	Yes
.21	-8	8	Yes	.19	-3	1	Yes
.18	-6	5	Yes	.08	-8	-4	No
.12	-8	3	Yes	.17	-8	0	Yes
.09	-5	-7	No	.16	-8	-4	Yes
.21	-6	4	Yes	.13	2	5	Yes
.24	-1	6	Yes	.15	-4	6	Yes
.17	-7	3	Yes	.17	-7	-5	Yes
.13	-8	3	Yes	.15	-7	1	Yes
.18	-8	-1	No	.12	-4	0	Yes
.29	0	7	Yes	.19	-8	1	Yes
.11	-1	5	Yes	.09	3	8	Yes
.28	-8	1	Yes	.14	-8	-5	No
.22	-4	7	No	.29	1	4	Yes
.19	-1	6	Yes	[Mean ρ = .18]			

* For Unique Peak results only

	$\overline{\Delta L}$	$\overline{\Delta C}$
MEAN*	-4.63	2.88
STD*	3.13	3.16

83% Successful

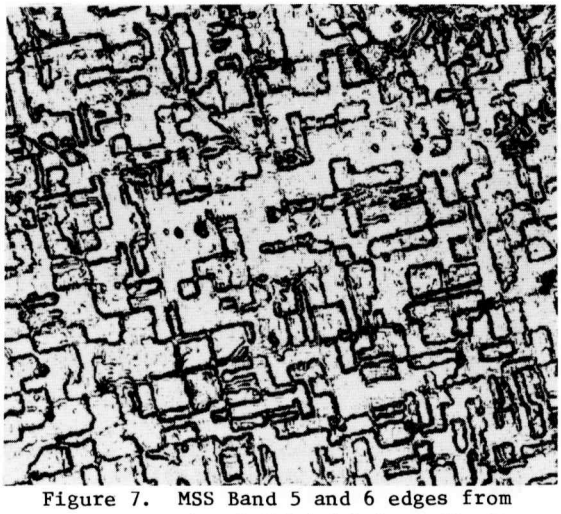

Figure 7. MSS Band 5 and 6 edges from thresholded Sobel gradient.

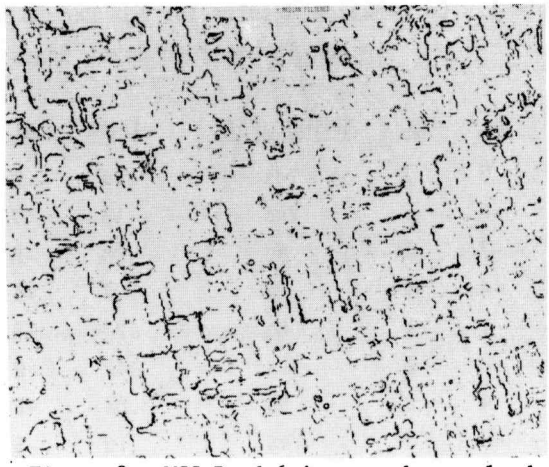

Figure 8. MSS Band 6 imagery deconvolved, interpolated to 19m, Sobel edge processed, and thresholded.

Table 3. Thresholded MSS Combined Bands 5 and 6 RBV Correlation Results.

ρMAX	ΔL	ΔC	ρMAX	ΔL	ΔC
.2	1	2	.11	1	-1
.09	2	4	.09	1	6
.08	--*		.09	--	
.09	-6	6	.10	4	-1
.16	--		.11	-5	-1
.07	5	2	.10	-7	-8
.12	--		.11	4	-2
.08	-6	6	.19	-5	7
.08	-6	6	.15	-2	3
.13	-3	0	.10	-1	3
.14	5	3		--	
.11	--		.12	0	0
.18	-1	6	.11	4	1
.17	1	3	.10	5	-3
			.11	-6	0

Line Mean	-.65	% Acceptable	79%
Col. Mean	1.83		
		Aver. ρMax	.12
Line Std. Dev.	4.16		
Col. Std. Dev.	3.51		

* Blank entries indicate shift was at limit of lags and considered nonacceptable.

Table 4. Correlation Results for RBV and IFOV Deconvolved MSS Band 6 Data. Thresholded Sobel Edges.

ρMAX	ΔL	ΔC	ρMAX	ΔL	ΔC
.29	-1	3	.29	1	5
.15	-2	-3	.10	5	6
.21	-6	6	.11	0	4
.18	-6	6	.37	-6	4
.17	8	-5	.20	-6	-1
.24	-3	7	.13	-2	2
.24	--		.19	--	
.21	-7	6	.18	-1	-1
.18	-6	6	.14	0	5
.17	-6	3	.15	--	
.31	--		.18	0	6
.16	-1	7	.26	--	
.19	-4	4	.25	-2	2
.26	-2	7	.32	2	7
.17	3	-3			

Line Mean	1.75	% Acceptable	83%
Col. Mean	3.46		
		Aver. ρMax	.21
Line Std. Dev.	3.74		
Col. Std. Dev.	3.55		